PERGAMON

Scripta Materialia 47 (2002) 817–823

Scripta MATERIALIA

www.actamat-journals.com

Microstructural evolution in electroplated Cu thin films

M.T. Pérez-Prado [a,*], J.J. Vlassak [b]

[a] *Department of Physical Metallurgy, Centro Nacional de Investigaciones Metalúrgicas (CENIM), CSIC Avda. Gregorio del Amo, 8, 28040 Madrid, Spain*

[b] *Division of Engineering and Applied Sciences, Harvard University, 311 Pierce Hall, 29 Oxford Street, Cambridge, MA 02138, USA*

Received 15 July 2002; received in revised form 23 July 2002; accepted 24 July 2002

Abstract

The microstructural evolution of electroplated Cu films (0.89 to 3.0 μm thick) has been studied by texture analysis. Before annealing, the volume fraction of (1 1 1) grains decreases with increasing film thickness, while that of (1 0 0), (1 1 0), and randomly oriented grains increases. Annealing causes a decrease in the ⟨1 1 1⟩ fiber intensity in the thinnest films due to growth of randomly oriented grains and multiple twinning.

Keywords: Thin films; Multiple twinning; Texture

1. Introduction

Copper has replaced aluminum as the main interconnect material since 1998 due to its high electrical and thermal conductivity, as well as a melting point that is almost twice that of aluminum [1]. The higher stiffness and yield strength of copper however may lead to elevated mechanical stresses as a result of temperature changes imposed on the copper metallization during microchip fabrication [2]. These stresses can cause problems during fabrication and may even impair the reliability of the microchip afterwards. Thus, a good understanding of the mechanical behavior will aid in the design of more robust devices.

Mechanical properties of thin films are strongly correlated with microstructural characteristics such as grain size, grain orientations and grain boundaries [3–5]. Thin film microstructure depends sensitively on the thermal history of the films. Annealing often leads to normal and abnormal grain growth due to the need to lower the total energy accumulated in the film [6–10]. The resulting equilibrium texture and grain size are determined by the relative magnitudes of the surface or interface energy, the grain boundary energy, and the strain energy. These quantities depend in turn on deposition parameters, substrate composition, film thickness, and thermal history of the film. The aim of this work is to investigate the effects of film thickness and thermal history on the microstructural evolution of copper thin films using texture analysis as the main characterization tool.

2. Experimental procedure

Copper films 0.89, 1.81, and 3.0 μm thick were deposited onto ⟨1 0 0⟩ Si single crystal substrates.

* Corresponding author. Tel.: +34-91-5538900; fax.: +34-91-534-7425.

E-mail address: tpprado@cenim.csic.es (M.T. Pérez-Prado).

1359-6462/02/$ - see front matter
PII: S1359-6462(02)00308-1

Bare Si substrates were first coated with a 1000 Å LPCVD SiN_x film and a 200 Å PVD TaN barrier layer. Cu films were then deposited to various thicknesses by means of a standard electroplating process used in the semiconductor industry [11,12]. Immediately prior to electroplating, a very thin Cu layer was sputter deposited onto the TaN to act as a seed layer for the electroplating process.

The films were annealed in vacuum (8×10^{-5} mbar) at 400 and 600 °C during 1 h. Film microstructure was analyzed in a JEOL SEM in the backscattered mode. X-ray texture analysis was performed in a Siemens D5000 diffractometer. An absorption correction was made to the measured X-ray intensities [13] since the X-ray penetration exceeded the film thickness. The macrotexture is represented by the orientation distribution function (ODF). X-ray peak analysis is performed using the software PeakFit™ 4.0. Volume fractions of material associated with specific texture components were calculated following the methodology described in [14]. The microtexture and grain sizes were measured using electron backscatter diffraction (EBSD) [15]. System software and hardware (EDAX/TSL) for microtexture measurement was installed on a Topcon SM-510 SEM at the Naval Postgraduate School in Monterey, California, USA. The microtexture is represented by the (1 1 1), (2 2 0), and (2 0 0) pole figures. Misorientation distribution histograms are used to show the grain boundary character.

3. Results

The microstructure of the electroplated Cu films was found to be highly dependent on film thickness. Fig. 1 shows the microstructure of Cu films, 3.0 μm (Fig. 1a), 1.81 μm (Fig. 1b), and 0.89 μm (Fig. 1c) thick. Using EBSD, the average grain size was measured to be approximately 1 μm in all films. Twinning as well as isolated abnormally grown grains, usually with a (1 0 0) orientation and about 6–8 μm in size, were observed in all films. It should be noted that the EBSD measurements do not distinguish between twins and regular grains and that twins are counted as separate grains.

The texture of the Cu films varies significantly with film thickness. As shown in Fig. 2, the texture of the 3.0 μm film is formed by ⟨1 1 1⟩, ⟨1 0 0⟩, and ⟨1 1 0⟩ fibers, as well as a strong random component. Fig. 2a shows a $\varphi_1 = 90°$ ODF section, in which the three fiber components are indicated. The maximum intensities corresponding to the ⟨1 1 1⟩, ⟨1 0 0⟩, and ⟨1 1 0⟩ fibers are 16, 8, and 5, respectively. The presence of a significant number of grains with random orientations can be appreciated in Fig. 2b, where the discrete (1 1 1), (2 0 0), and (2 2 0) pole figures derived from the EBSD measurements have been represented. Good agreement between the micro- and macrotextures indicates that there is no significant texture gradient across the film thickness. The misorientation distribution histogram depicted in Fig. 2c is formed by the superposition of a distribution close to that predicted by Mackenzie [16] for a random distribution of cubes (see inset) and an excess of 60° ⟨1 1 1⟩ ($\Sigma = 3$) coherent twin boundaries. The latter have low energy and very low mobility. Approximately 40% of the boundaries are coherent twin boundaries.

As the film thickness decreases, the ⟨1 1 1⟩ fiber becomes stronger and the random component

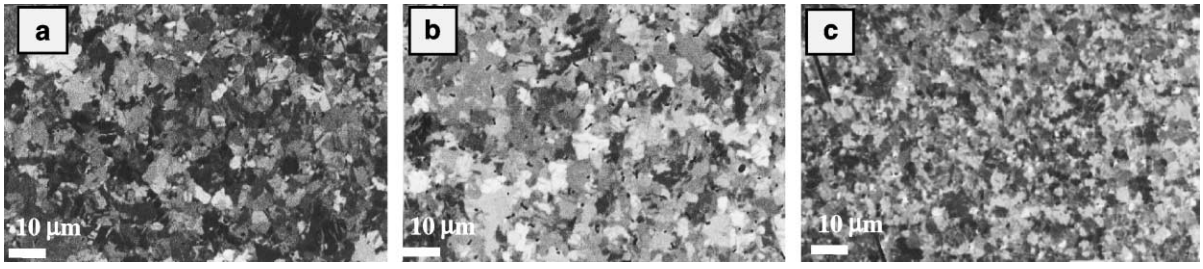

Fig. 1. SEM micrographs showing the microstructure of the Cu films after deposition. BSE imaging mode. (a) 3.0 μm; (b) 1.81 μm; (c) 0.89 μm.

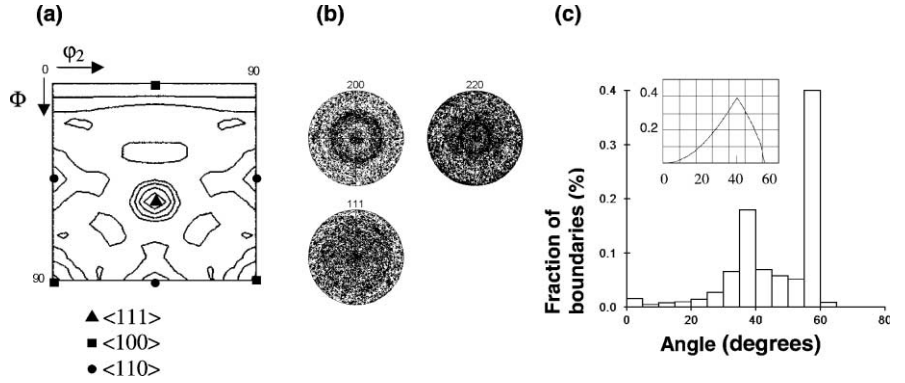

Fig. 2. Texture of the 3.0 μm Cu film. (a) Macrotexture: $\varphi_1 = 90°$ section of the ODF (levels: 1, 4, 8, 12, 16); (b) Microtexture: (2 0 0), (2 2 0), and (1 1 1) discrete pole figures; (c) Misorientation distribution histogram.

decreases. Fig. 3 shows the texture of the 0.89 μm film, which is clearly dominated by a sharp ⟨1 1 1⟩ fiber. The predominance of ⟨1 1 1⟩ oriented grains can be appreciated in Fig. 3a, in which the macrotexture of the 0.89 μm film has been represented by means of a $\varphi_1 = 90°$ ODF section. The intensity of the ⟨1 1 1⟩ fiber component has increased with respect to that of the 3.0 μm film (Fig. 2), reaching a value of 32. The intensities of the ⟨1 0 0⟩ and ⟨1 1 0⟩ fiber components are now 8 and 3, respectively. The predominance of the ⟨1 1 1⟩ fiber component results in a concentration of poles at 0° and a sharp ring at 70° in the (1 1 1) pole figure. In the (1 0 0) pole figure, a ⟨1 1 1⟩ fiber texture gives rise to a ring of uniform pole concentration at 54°, and in the (1 1 0) pole figure rings appear at 35° and 90°. The boundary misorientation distribution (Fig. 3c) resembles that of a fiber texture with excess twin boundaries. In a histogram for a perfect fiber texture, the fraction of boundaries is constant over the entire misorientation range and approximately equal to 8%. In addition to the misorientation due to the fiber texture, there is also a peak at 60° due to ⟨1 1 1⟩ ($\Sigma = 3$) coherent twin boundaries. Coherent twin boundaries make up approximately 20% of all boundaries in this film. The lower incidence of twins in the thinner films explains the apparent discrepancy between the EBSD grain sizes and the micrographs in Fig. 1. Since the EBSD measurements count twins and since the number of twinned grains increases with film thickness, the actual grain size as apparent in Fig. 1 may increase with film thickness, while the EBSD measurements remain largely unchanged.

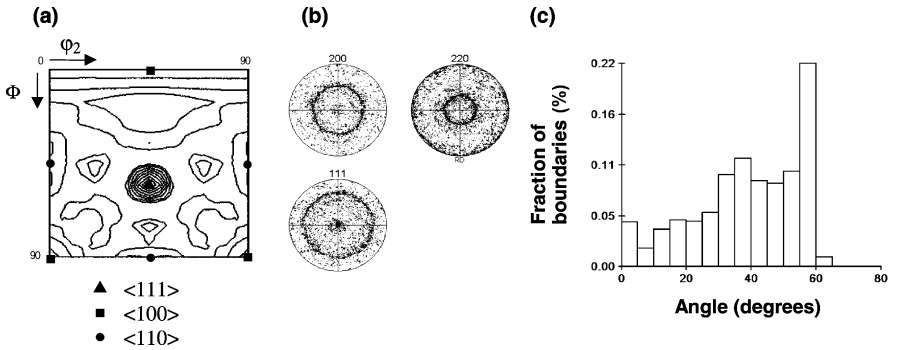

Fig. 3. Texture of the 0.89 μm Cu film. (a) Macrotexture: $\varphi_1 = 90°$ section of the ODF (levels: 1, 4, 8, 12, 16, 20, 24, 28, 32); (b) Microtexture: (2 0 0), (2 2 0), and (1 1 1) discrete pole figures; (c) Misorientation distribution histogram.

Table 1
Volume fraction of the ⟨1 1 1⟩ fiber texture before and after annealing at 600 °C for 1 h

	Thickness (μm)		
	0.89	1.81	3.0
Before anneal	58	42	30
After anneal	52	40	31

The volume fraction of (1 1 1) oriented grains is listed in Table 1 as a function of film thickness.

Normal grain growth was observed in all films after annealing. Fig. 4 clearly shows that grain size increases with film thickness for a given set of annealing conditions. Average values of 5.72, 5.67, and 1.57 μm were measured for the 3, 1.81, and 0.89 μm thick films, respectively, after a 1 h anneal at 600 °C (Fig. 4). The abnormal grains grow only slightly, reaching sizes of approximately 8–9 μm. For a given film thickness, grain size increases with annealing temperature. Twinning is apparent in all annealed films. Annealing also results in a weakening of the ⟨1 1 1⟩ fiber texture in the thinner films. No changes were detected in any of the other fiber components. The volume fraction of (1 1 1) oriented grains after annealing is summarized in Table 1.

4. Discussion

The present results demonstrate that the texture of electroplated Cu films varies significantly in the 0.89 to 3.0 μm thickness range. In the thinnest films, a strong ⟨1 1 1⟩ fiber texture is present. As the film thickness increases, the volume fraction of (1 1 1) grains decreases and that of (1 0 0), (1 1 0), and randomly oriented grains increases. This loss of ⟨1 1 1⟩ texture with increasing film thickness has been reported previously for electroplated Cu films by Walther et al. [17].

Thin electroplated coatings of fcc metals usually have a ⟨1 1 1⟩ fiber texture [17,18], since the (1 1 1) close-packed surface in these materials is associated with the lowest surface free energy. The residual stress in a coating and the associated strain energy, however, provide a driving force for the formation of texture components with a higher in-plane compliance [6]. This follows directly from the elastic anisotropy of Cu and from the fact that (1 1 1) grains have the lowest in-plane compliance of all possible orientations. Formation of more compliant texture components can happen during deposition, but also during the subsequent recrystallization often observed in electroplated Cu thin films. When the Cu films are first electroplated, the grain size is extremely small (~0.1 μm). This microstructure is not stable and the film recrystallizes at room temperature for several days after deposition [17,19–21]. During this recrystallization, new low-compliance texture components can develop via several mechanisms: normal growth of small randomly oriented grains at the expense of (1 1 1) grains, abnormal growth of grains with a high-compliance orientation such as (1 0 0) [6], and twinning of (1 1 1) grains [17]. After recrystallizing, the Cu coatings in the current investigation have a residual stress of approximately

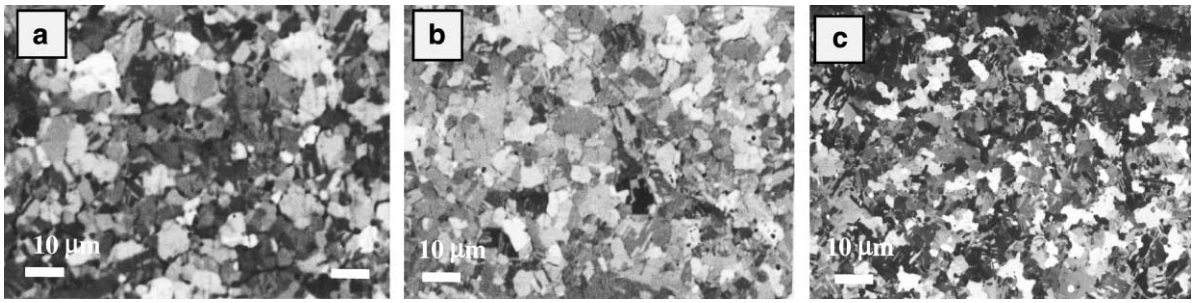

Fig. 4. SEM micrographs showing the microstructure of the Cu films annealed at 600 °C for 1 h. BSE imaging mode. (a) 3.0 μm; (b) 1.81 μm; (c) 0.89 μm.

110 MPa. The effect of film thickness in these coatings can then be understood by realizing that the strain energy in the film and thus the driving force for the formation of texture components with lower in-plane compliance increases with increasing film thickness. Assuming an energy difference between the (1 0 0) and (1 1 1) surfaces of approximately 13 mJ/m^2 [22] and taking the energy of the interface equal to that of the surface, we estimate that (1 0 0) oriented grains are favored over (1 1 1) grains if the film thickness exceeds 0.6 μm. Based on this calculation one could expect abnormal grain growth in all samples, as is indeed observed. The critical coating thickness for twinning is approximately 2.5 μm. Although other factors such as grain boundary energy should be taken into account to obtain a more accurate result, the critical thickness calculation suggests that twinning is also a viable mechanism for the formation of new texture components in these films and may explain the big difference in the number of coherent twin boundaries observed as a function of film thickness.

We have observed that upon annealing the volume fraction of (1 1 1) grains decreases slightly in the thinnest films, while it remains largely unchanged in the other films (Table 1). No other texture components are strengthened. This may be explained by the fact that the residual stress in unpassivated Cu films relaxes very quickly at high temperatures [5], thus reducing the driving force for developing more compliant texture components. The present results do suggest a small increase of randomly oriented grains upon annealing in the thinnest film. This texture randomization may be attributed to two factors: (a) nucleation and/or growth of randomly oriented grains at the expense of (1 1 1) grains or (b) multiple twinning [23–25] of (1 1 1) grains during growth. According to Tracy and Knorr [26], twinning can be detected through analysis of the (1 1 1) pole figure intensity profile. Fig. 5a shows the (1 1 1) intensity profiles corresponding to films of 0.89 μm thickness, both before and after annealing at 600 °C for 1 h. According to [26], a ⟨1 1 1⟩ fiber texture produces peaks at 0° and 70.5°. Single twinning of the (1 1 1) grains gives rise to the (5 1 1) component. Peaks for this orientation can be found at 38.2°, 56.2°, and at 70.5°. Multiple twinning results in orientations like (1 1 2), (5 7 13), and (2 2 5), which give peaks around 20° and 50°. The presence of a (1 0 0) fiber texture gives a peak at 54.7°, and a (1 1 0) fiber texture results in a peak at 35°. Thus, the difficulty in detecting twinning lies in that some of the peaks overlap (e.g. 38.2° (5 1 1) and 35° (1 1 0); 56.2° (5 1 1) and 54.7° (1 0 0)) and therefore a detailed analysis is needed in order to evaluate volume fractions of twinned material. However, no overlapping occurs at the ∼20° peak, which corresponds to grain orientations resulting from multiple twinning. This peak has been detected in all as-deposited and annealed samples. The volume fraction of the multiply twinned grains before and after annealing was calculated from the

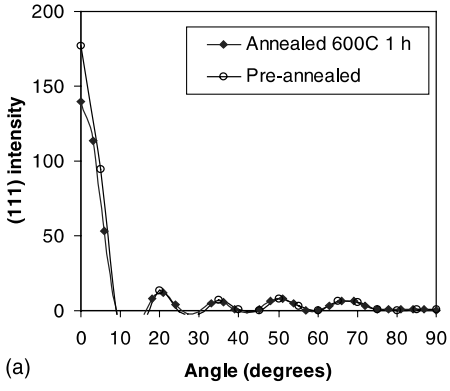

(a)

Thickness (μm)	As-deposited films (%)	Annealed films (%)
3.0	18	20
1.81	20	24
0.89	18	24

(b)

Fig. 5. (a) Radial intensity profile of the (1 1 1) pole figure for a 0.89 μm Cu film, both as-deposited and annealed at 600 °C for 1 h. (b) Volume fraction of multiply twinned grains (in %).

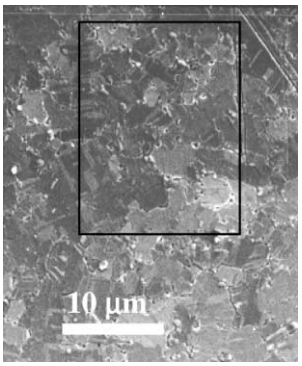

Fig. 6. Secondary electron SEM image showing boundary grooving in the 0.89 μm film annealed at 600 °C for 1 h. The inset indicates regions with a high concentration of twins, without (visibly) grooved boundaries.

appropriate (1 1 1) pole figures according to the methodology described in [14]. The results are listed in Fig. 5b. The volume fraction of multiply twinned grains in the thinnest film increases slightly after annealing. Thus, as suggested in [27], multiple twinning is indeed partially responsible for the decrease in the (1 1 1) texture observed in the thinnest film.

Annealing results in substantial normal grain growth. Relaxation of the residual stress at elevated temperature however reduces the driving force for abnormal grain growth. Additionally, grain boundary grooving, which occurs preferentially at high angle boundaries [1], may also hinder the growth of (1 0 0) grains [28]. These grains are most probably surrounded by high angle boundaries since the texture is dominated by (1 1 1) grains. Grain boundary grooving and twinning are indeed clearly visible in Fig. 6 showing a 0.89 μm film annealed at 600 °C for 1 h. Twin boundaries are not (visibly) grooved. Voids can also be observed at the grain boundaries.

5. Conclusions

The effect of film thickness on the microstructural evolution of Cu thin films of 0.89, 1.81, and 3.0 μm thickness has been investigated by means of texture analysis. The following conclusions may be drawn from this study:

1. The texture of the as-deposited films is highly dependent on film thickness. In the thinnest films (0.89 μm), a strong ⟨1 1 1⟩ fiber texture is present. The volume fraction of (1 1 1) grains decreases with increasing film thickness while that of (1 0 0), (1 1 0), and randomly oriented grains increases. All films have a bimodal grain size distribution with a small number of giant grains, 6–8 μm in size, providing clear evidence for abnormal grain growth. The average grain size of all films is independent of film thickness and approximately equal to 1 μm. These observations are consistent with predictions based on a strain energy minimization model.
2. All films show significant normal grain growth on annealing. No significant increase in abnormal grain growth is observed. This is consistent with relaxation of the film stress at elevated temperature. Annealing leads to texture randomization in the thinnest films, while the texture remains almost unchanged for the 1.81 and 3.0 μm films. Texture randomization in the thinnest films can be attributed to growth of randomly oriented grains and multiple twinning.

Acknowledgements

T.R. McNelley and D.L. Swisher, from the NPS in Monterey, CA, are greatly appreciated for assistance with microtexture measurements. Funding from the NSF (DMR-0133559), the Harvard Division of Engineering and Applied Sciences, and from the R&C program (MCT-Spain) is acknowledged.

References

[1] Weiss D. PhD Dissertation, Max-Planck Institut für Metallforschung, Stuttgart, 2000.
[2] Vinci RP, Zielinski EM, Bravman JC. Thin Solid Films 1995;262:142–53.
[3] Nix WD. Metall Trans A 1989;20:2217–45.
[4] Baker SP, Kretschman A, Artz E. Acta Mater 2001;49:2145–60.
[5] Vinci RP, Vlassak JJ. Ann Rev Mat Sci 1996;26:431–62.

[6] Thompson CV, Carel R. J Mech Phys Solids 1996;44(5): 657–73.
[7] Greiser J, Müller D, Müllner P, Thompson CV, Artz E. Scripta Mater 1999;41(7):709–14.
[8] Zielinski EM, Vinci RP, Bravman JC. Appl Phys Lett 1995;67(8):1078–80.
[9] Frost HJ, Thompson CV, Walton DT. Acta Metal Mater 1990;38(8):1455–62.
[10] Frost HJ, Thompson CV, Walton DT. Acta Metal Mater 1992;40(4):779–93.
[11] Brongersma SH, Richard E, Vervoort I, Maex K. Institute of Electrical & Electronics Engineers 2000:31–3.
[12] Lee H, Lopatin D, Wong SS. Institute of Electrical Electronics & Engineers 2000:114–6.
[13] Shultz LG. J Appl Phys 1949;20:1030–3.
[14] Hong SH, Chung KH, Lee CH. Mater Sci Eng 1996; 206:225–32.
[15] Randle V. Microtexture determination and its applications. The Institute of Metals; 1992.
[16] Mackenzie JK. Biometrica 1958;45:229.
[17] Walther D, Gross ME, Evans-Lutterodt K, Brown WL, Oh M, Merchant S, Naresh P. In: Mater Res Soc Symp Proc 612, 2000. D10.1.1-10.
[18] Pangarov NA. J Electr Chem 1965;9:70–85.
[19] Harper JME, Cabral Jr C, Andricacos PC, Gignac L, Noyan IC, Rodbell KP, et al. J Appl Phys 1999;86(5):2516–25.
[20] Tomov IV, Stoychev DV, Vitanova IB. J Electrochem Soc 1985;15:887.
[21] Jiang Q-T, Smekalin K. In: Sandhu GS, Koerner H, Murakami M, Yasuda Y, Kobayashi N, editors. Adv Metalliz Conf 1998. Pittsburgh, PA: Mater Res Soc; 1999. p. 209–15.
[22] Zielinski EM, Vinci RP, Bravman JC. Appl Phys Lett 1995;67:1078–80.
[23] Haessner F. Recrystallization of metallic materials. Riederer-Verlag Gmbh; 1978.
[24] Humphreys FJ, Hatherly M. Recrystallization and related annealing phenomena. Pergamon Press; 1995.
[25] Berger A, Wilbrandt PJ, Ernst F, Klement U, Haasen P. Progr Mater Sci 1988;32:1–95.
[26] Tracy DP, Knorr DB. J Electr Mater 1993;22(6):611–6.
[27] Lingk C, Gross ME, Brown WL. J Appl Phys 2000; 87(5):2232–6.
[28] Mullins WW. Acta Metall 1958;6:414.